Journal of the Electrochemical Society, Vol., 142, No.7, 1995, pp2290-2295.
ISSN: (Print 0013-4651) (Online 1945-7111)
DOI: 10.1149/1.2044289
http://www.electrochem.org/
http://scitation.aip.org/JES
http://scitation.aip.org/getpdf/servlet/GetPDFServlet?filetype=pdf&id=JESOAN000142000007002290000001&idtype=cvips&prog=normal
© The Electrochemical Society, Inc. 1995. All rights reserved. Except as provided under U.S. copyright law, this work may not be reproduced, resold, distributed, or modified without the express permission of The Electrochemical Society (ECS). The archival version of this work was published in Journal of the Electrochemical Society, Vol., 142, No. 7, 1995, pp2290-2295.

Repassivation Transients Measured with the Breaking-Electrode Technique on Aluminum Thin-Film Samples

G. S. Frankel,[a] C. V. Jahnes,[b] V. Brusic,[b] and A. J. Davenport[b]
[a]IBM Research Division, T. J. Watson Research Center, Yorktown Heights, New York
[b]Brookhaven National Laboratory, Upton, New York

ABSTRACT

The breaking-electrode technique was used to study repassivation transients of small, fresh metal areas of Al exposed to a conductive electrolyte at a range of potentials. The peak current density measured within the first few microseconds after breaking was found to be ohmically limited, with an ohmic resistance that is substantially higher than that measured minutes after breaking. The current decay during the first 3 s was recorded and found to be exponential in nature. By plotting the data as log i *vs.* $(it)^{-1/2}$, it is concluded that oxide growth was better.represented by the direct logarithmic law than by high-field kinetics. Cathodic current transients having a complex shape Were observed at low potentials. It is suggested that oxide growth at potentials slightly above the reversible potential for oxide formation retards the water reduction reaction. The advantages and limitations of the breaking-electrode technique are discussed.

Introduction

Three years ago we described the breaking-electrode technique for studying passivity on the microsecond time scale.[1] By breaking a thin metallic film deposited on an insulating substrate, a very small fresh metal area (the sample cross section) is created very quickly. In the earlier communication, the influence of covering the passive film near the freshly created metal surface was investigated. It was shown that a 1000 Å thick coating of sputtered SiO_2 greatly reduced the artifact associated with capacitative discharging of the nearby passive film, resulting in much larger measured initial current densities compared to the case with no sputtered oxide on the passive film.

Others have studied the early stages of passivation by breaking tensile samples,[2-5] scratching with a stylus,[8-10] or slicing with a steel guillotine blade.[11,12] The scratching technique is complicated by the fact that fresh metal area is created sequentially, so that the fresh area first formed undergoes significant passivation during the time that the end of the scratch is still being formed. It is not possible to examine times less than about 1 ms using the scratching and guillotining techniques. Tensile samples can be broken quickly, but it is difficult to work with samples of extremely small cross sections, and the currents generated from samples with large cross sections result in very large ohmic resistance drops in the electrolyte. By creating an extremely small area very quickly, the breaking-electrode technique overcomes some of the problems inherent with the other techniques.

In this work the breaking-electrode technique is further developed. Both the peak current

densities and extended current-decay regions are examined. The utility and limitations of the technique are probed.

Experimental

Much of the experimental approach is similar to that described in the earlier work.[1] In order to improve the reproducibility of the breaks, Si substrates were used instead of glass; Si wafers with a [100] orientation cleave easily along <110> directions. In order to insulate the metal film from the Si substrate, wafers covered with 1 μm of thermal oxide were used. It was found that thinner oxides had sufficient leakage to effectively connect the metal film to the Si, thereby confusing the data interpretation. Al stripes, 6.35 mm wide, were sputter-deposited on top of the oxide-covered Si in an Ar plasma through a physical mask to a thickness of about 1500 Å, giving a cross-sectional area of 9.5×10^{-6} cm^2 upon breaking. A 600 Å layer of Si_3N_4 was deposited on top of the Al stripes to reduce capacitative discharging of the top surface immediately after the break.[1] Note that silicon oxide was used in. the previous work; any insulating thin film can be used for this purpose. Figure la shows a schematic cross section of the sample.

The wafers were first separated into pieces about 1.2 cm wide, each containing one metal stripe. The samples were inserted through a slot in the wall of a small Plexiglas cell (40 ml) and clamped by pressing on the substrate area adjoining the stripe, Fig. lb. Since the sample was not clamped by pressing on the metal area, there was no chance to scratch through the nitride overcoat by doing so. The sample extended into the cell about 4 mm over the edge of the clamp. A slot in the clamp resulted in approximately 0.32 cm^2 of nitride-covered top metal area being exposed to the solution after the break. A scribe mark, made with a diamond stylus on the substrate to one side of the metal stripe, was aligned with the edge of the clamp to facilitate crack initiation when the cantilevered portion of the sample was tapped with a Plexiglas plunger. A mercurous sulfate (MSE) reference electrode and Au foil counterelectrode were immersed in the cell at a distance from the sample. All potentials are referred to the MSE scale.

The potential was controlled, and the current was measured, with an EG&G PAR 173 potentiostat containing a Model 179 coulometer plug-in. The cell and potentiostat electrometer unit were placed into a metal can, which acted as a Faraday cage. A hole cut into the top of the can allowed access to the plunger for breaking. Data were collected with both a Nicolet 4094A/4562 digital oscilloscope and an HP 345 8A multimeter. The oscilloscope collected data at 0.5 μs/point with a 12 bit resolution. The multimeter has 16 bit resolution and was typically set to collect data at 0.1 ms/point and 100 mV full scale. The data from the oscilloscope and multimeter were pieced together to form a single transient by offsetting the time associated with the multimeter data so that the first few points overlapped the oscilloscope data in that time range. This was necessary because of a difference in the exact triggering time of the two devices. When measuring a low current on a coarse scale, there will be an offset. The offset in the multimeter data was compensated following collection of the data by subtracting the difference of the steady-state value measured with the current range used during the transient measurement (1 or 10 mÅ full scale) and that measured at the lowest possible range (1 μA full scale).

The solution resistance was determined for some electrolytes on samples after a break by electrochemical impedance spectroscopy (EIS) using an EG&G PAR 273 potentiostat and a Schlumberger 1255 frequency response analyzer.

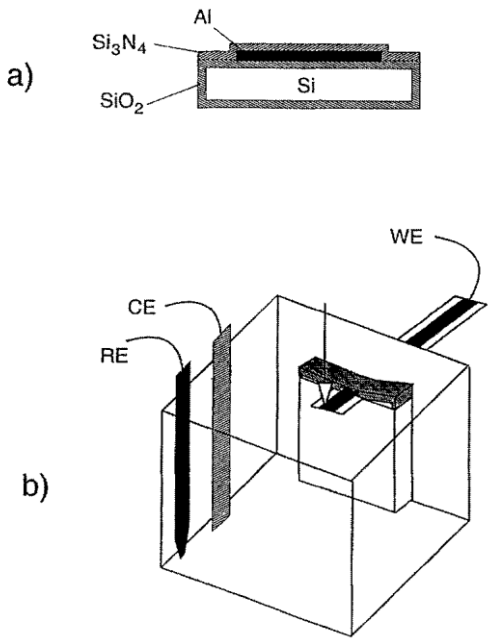

Fig. 1. Schematic diagrams of (a) sample cross section and (b) breaking-electrode cell.

Results and Discussion

Anodic transients.—The initial part of a typical transient is shown in Fig. 2. This transient is for a sample held at 0 V MSE in 1.2*N* K_2SO_4. The current reaches a maximum of about 7 mA within a few microseconds, and then decays rapidly. When normalized for the cross-sectional area, the peak current represents a current density of about 700 A/ cm^2. This result is similar to data reported previously under the same conditions.[1] Also shown in Fig. 2 is the potential monitored from the potentiostat electrometer. For this experiment the potentiostat full-scale current value was 10 mA (100 Ω resistor), and the potential oscillates slightly about the control potential during the current transient. This small deviation is negligible, especially compared to the large ohmic potential drop generated during this time, as will be discussed below.

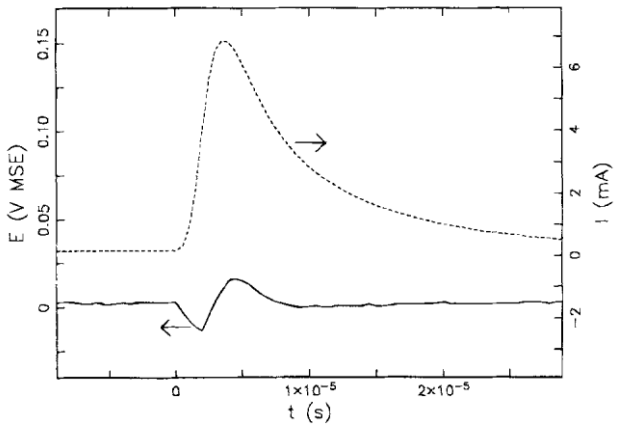

Fig. 2. Initial current and electrometer potential transients for sample held at nominal potential of 0 V MSE in 1.2*N* K_2SO_4.

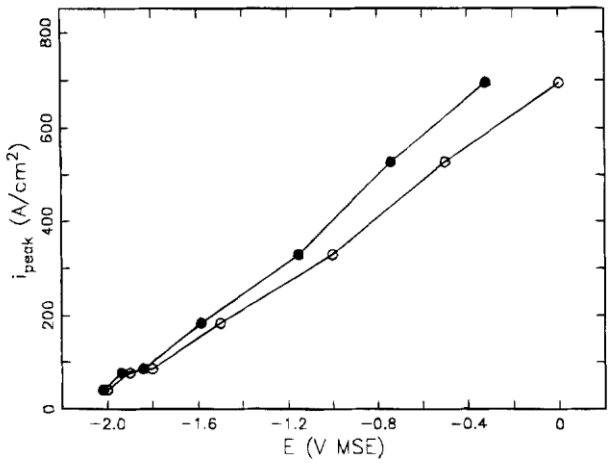

Fig. 3. Peak current density as a function of potential for Al in 1.2*N* K_2SO_4. Open symbols, uncorrected, and filled symbols, IR-corrected using measured resistance of 49 Ω.

The open circles in Fig. 3 are the averages of peak current values from several experiments at potentials in the range −2.0 V to 0 V MSE, which resulted in positive peak values. Peak current is linearly dependent on applied potential, indicating that the rate of reaction is ohmically limited. This assessment is further supported by the observation that the peak current at a given potential (−1.5 V MSE) in a variety of solutions is proportional to the conductivity and independent of pH over a range where it would be expected that pH should have an effect on dissolution kinetics, Fig. 4. It is interesting to note that Fig. 4 also indicates that any pH change that might be occurring near the sample surface in the period immediately after the break does not affect the signal, likely because of the overriding ohmic effects.

The concentration of current flowing in the electrolyte from the distant counterelectrode to the small fresh metal surface results in an approach resistance and ohmic potential drop in the electrolyte. Most of this potential drop will occur in the region very close to the sample surface. The electrolyte ohmic resistance was determined several minutes after breaking by the high frequency impedance limit. For samples in 1.2*N* K_2SO_4, which is close to saturation with conductivity 0.091 ft^{-1} cm^1, the ohmic resistance was found to be 49 ft. The ohmic resistance measured in all solutions was about half the value given by a theoretical expression derived for the resistance associated with rectangular electrodes, which has been successfully applied to scratched electrodes.[13] This difference may be due to the fact that the line of fresh metal in the broken electrode is not in an infinite insulating plane; the current has greater access to the freshly exposed area of the broken electrode.

The measured ohmic resistance is much smaller than the resistance that can be determined from the slope of the *i-E* curve, 273 Ω. Correspondingly, peak current is still linearly dependent on potential following correction of the applied potential for IR drop using the measured value of resistance, 49 Ω (the filled circles in Fig. 3). There are various possible explanations for why the IR-corrected data do not exhibit Tafel-type kinetics. Charging of the double layer of the fresh metal area is a nonfaradaic effect that may play a role. However, the charges measured in the first few microseconds far exceed any reasonable estimate of the double-layer charge. It should be realized that the maximum current value is not a steady-state measurement. It is the point at which the rate of current increase from the exposure of fresh area

to the electrolyte is balanced by the effect of current decrease from passivation. As a result of this balance, perfect Tafel behavior should not necessarily be expected.

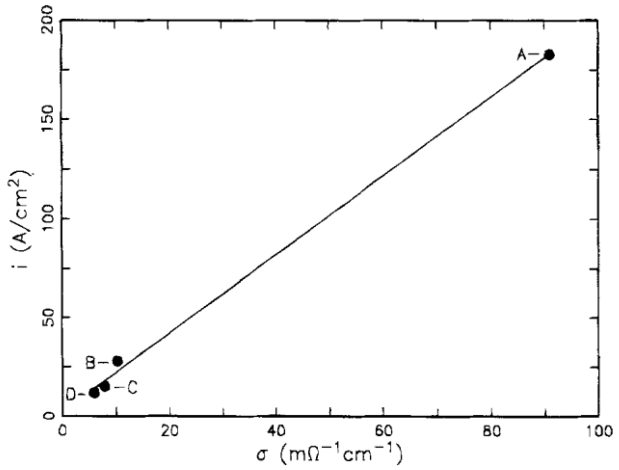

Fig. 4. Peak current density as a function of electrolyte conductivity for Al at -1.5 V MSE: (a) 1.2N K_2SO_4, pH 5.6; (b) 0.1*N* K_2SO_4, pH 6; (c) 0.1*N* Na_3PO_4, pH 12; (d) 0.1*N* $Na_2B_4O_7$, pH 9.2.

It is possible, however, that the actual resistance during the initial microseconds of the break is larger than that measured afterwards, perhaps because of blocking of the fresh metal area by the broken-off piece before it falls away into the cell. The maximum observed velocity of cracks in elastic materials is about one-half the theoretical limit, the Rayleigh wave speed in that material.[14] Assuming that the cleavage crack in the Si substrate has a velocity of 3000 m/s (approximately one-half the speed of sound in Si), it would take about 2 μs for a crack to propagate along the 6.4 mm wide Al stripe. This roughly corresponds to the time at which the current maximum is observed (3 to 10 μS). In order for the broken-off piece to move away from the surface a distance equal to three times the thickness of the film, it would need to travel at about 20 cm/s during the first 2 μs. It is reasonable to suggest that the broken-off piece moving away in the aqueous solution blocks the access of current to the fresh metal area resulting in a larger ohmic resistance during the first few microseconds compared to that measured after the broken off piece sinks to the bottom of the cell.

Since the ohmic resistance at the time of the peak current is unknown, the peak-current/potential data cannot be accurately corrected for the ohmic potential drop. As mentioned above, the measured peak current might not exhibit Tafel behavior. Nonetheless, for purely illustrative purposes it is instructive to estimate the ohmic resistance by finding the value that, upon correction of the data, results in the best fit to a semilogarithmic relationship. This is shown in Fig. 5; the best fit was given by a value of 245 Ω, which is a large fraction of the total resistance. The resulting slope, about 400 mV/dec, is still quite large for a Tafel slope. The difference in potential for the two curves in Fig. 5 is the ohmic potential drop at the time of the maximum current. This value is about 1.6 V for the experiment controlled at 0 V. The 20 mV loss of control by the potentiostat is very small compared to this ohmic potential drop. At lower potentials, the ohmic potential drop was smaller, but the potentiostat oscillation was correspondingly lower also. The estimate of the ohmic resistance at very short times described above also illustrates the magnitude of the anodic reaction on bare Al that may be possible with small overpotentials in the absence of an ohmic potential drop. However, as will be described

below, ohmic effects are impossible to remove in the case of Al.
The decay portions of the anodic current transients over an extended time period were examined in a separate set of experiments from those used to study the peak current values. For these experiments the potentiostat full-scale current value was set to 1 mA (1000 Ω resistor). Since the peak current measured within a few microseconds with a 10 mA full-scale value (100 Ω resistor) was in the range of 1 to 7 mA, the potentiostat was overloaded during the initial part of the transient when the lower current range was used. In an experimental identical to that of Fig. 2, except with the larger resistor, the potential fluctuation was found to be about ±40 mV, and last about 30 μs. Current transients for the two current ranges are given in Fig. 6 for experiments at 0 V. The overload condition for the 1 mA full scale condition led to current oscillations during approximately the first 40 μS. However, at times greater than about 0.1 ms, the two curves practically overlie each other. This coincidence provides justification for using transients taken at 1 mA full scale to study the long-term (>0.1 ms) current decays. Because of the improved resolution, these transients extend to lower currents and longer times before merging with the background.

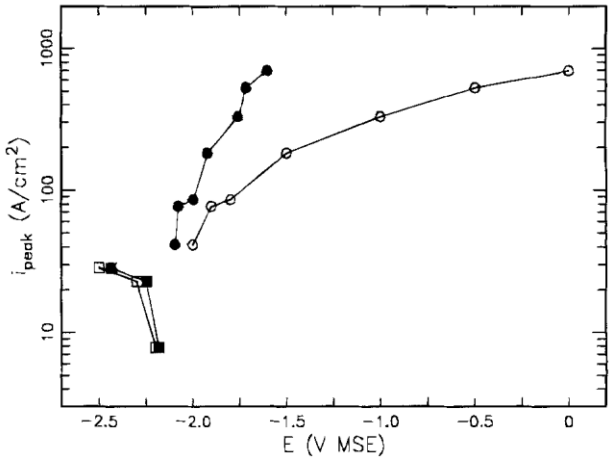

Fig. 5. Peak current density as a function of potential for Al in 1.*2N* K_2SO_4. Open symbols, uncorrected, and filled symbols, corrected with resistance that resulted in best fit to a straight line.

As is seen in Fig. 6, the current decay after the oscillations die out is linear in the log-log plot. The transients were fitted to the equation $i = At^b$, and the fitted lines (to simplify viewing) are shown in Fig. 7 for transients collected over a range of potentials. It should be noted that the fitted lines are quite good representations of the data as the values of r^2 were in the range of 0.981 to 0.997. The values of b were very close to −1 for all potentials (in the range −0.98 to −1.03), and the values of A were linearly dependent on potential, Fig. 8. Interestingly, the extrapolation of this curve intersects the potential axis at −2,15 V, which is very close to the intersection of the peak current *vs.* potential curve at −2.09 V.

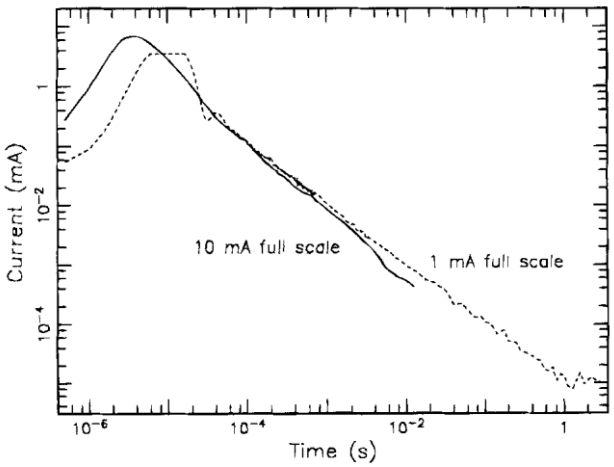

Fig. 6. Full current transients for samples held at 0 V MSE in 1.2N K_2SO_4, but with different full-scale current values (resistors): solid line, 10 mA (100 Ω); dashed line, 1 mA (1000 Ω).

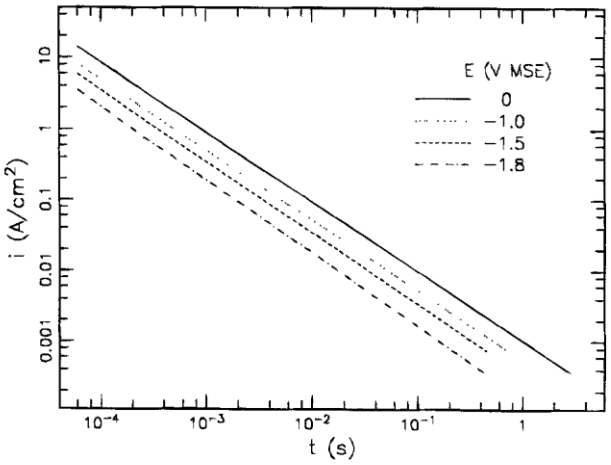

Fig. 7. Lines fitted to extended current decays at different potentials in 1.2*N* K_2SO_4.

There are two major models proposed for film growth under high electric field: the Cabrera-Mott model describing ion migration under a high field[15] and the place exchange model that yields "direct logarithmic" kinetics.[16] It is very difficult to distinguish which of the two models best fits kinetic passivation data.[17] Direct logarithmic kinetics predict a slope of exactly −1 for a plot of log *i vs.* log *t*,[17,18] whereas Cabrera-Mott high-field kinetics should yield a very slightly curved plot with a negative gradient of magnitude slightly less than 1[18] It has been shown that the plot of the log of the current density *vs.* the quantity $(it)^{-1/2}$ clearly identifies the effect of ohmic resistance on the current decay, and distinguishes the growth kinetics by the slope; a finite positive slope is predicted for the high-field model, and an infinite slope is predicted for direct logarithmic decay.[18] Figure 9 shows this plot for the transient in Fig. 6 that was taken with 1 mA full scale at 0 V in 1.2*N* K_2SO_4. The oscillations at the top of the curve reflect the oscillations in current at short times under these conditions. However, the region from 10 to 0.01 A/cm^2 is almost exactly vertical, corresponding to the fact that the current decays with t^{-1}. The region of the curve below 0.01 A/cm^2 may exhibit a positive slope although the noise at

the end of the transient is too great to determine this unambiguously. The infinite slope suggests that during Al repassivation, at least down to 0.01 A/cm^2, the film growth kinetics are better represented by a direct logarithmic rate law than by high-field kinetics.

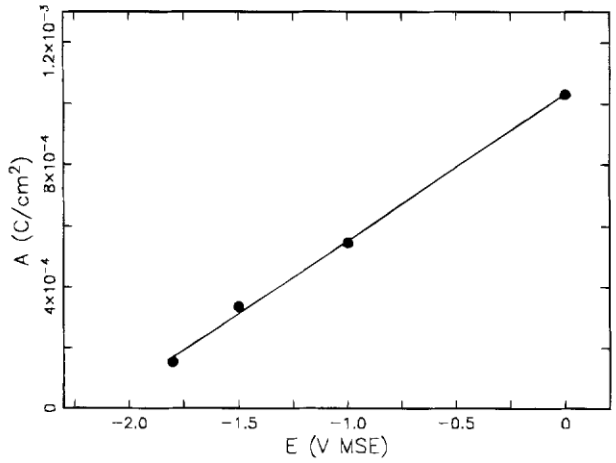

Fig. 8. Variation of factor A (from the fitted lines of the form $i = At^b$) with potential.

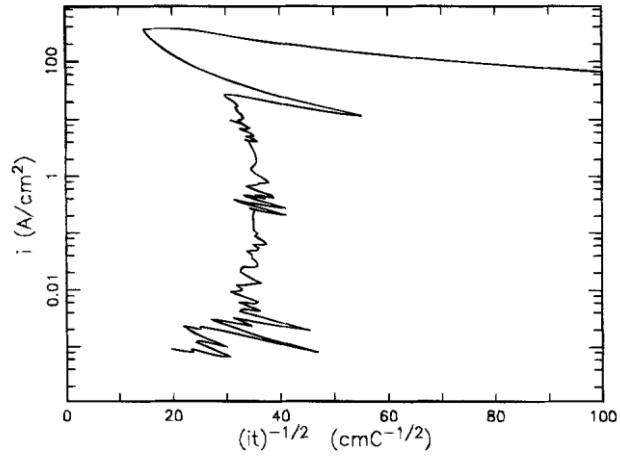

Fig. 9. Log i *vs.* $(it)^{-1/2}$ for Al at 0 V MSE in I.2N K_2SO_4.

The charge passed can be related to oxide film thickness with a few assumptions in order to check that the very large peak currents measured do not lead to unreasonable thicknesses. For the case of −1.0 V in 1.2 N K_2SO_4, approximately 6.9 mC/cm^2 is passed in the first 11 ms. (Note that the most charge that might be associated with the formation of the new double layer is about 0.1 mC/cm^2.) The current efficiency for oxide formation is not clear. However, if it is assumed that all of the oxidized Al remains in the oxide film, the film thickness can be estimated. Assuming 100% current efficiency, the 6.9 mC/cm^2 is equivalent to a 47 or 61 A film thickness, for the formation of AlOOH or $A1_2O_3$, respectively. Hydrogen evolution would lower the net anodic current leading to an underestimate of the passive-film thickness.

Cathodic Transients

Samples held at potentials in the range −2.2 to −2.5 V exhibited an initial cathodic peak, and these values are reflected in Fig. 5. (At potentials below −2.5 V, the Si_3N_4 overcoat appeared to break down as vigorous bubbling was observed on the sample top surface prior to breaking.) The initial portions of the transients at low potentials are rather complex, Fig. 10. Upon breaking, the current jumps to a negative value, increases rapidly to a positive peak, decreases to a second negative peak, and then slowly decays to smaller negative values. This may be viewed as a superposition of two responses, one anodic and one cathodic. The observation of an anodic signal in the middle of a cathodic transient suggests that the cathodic response increases faster and decays more slowly than the anodic reaction. It is not surprising that an anodic reaction is observed since the equilibrium potential for the $A1/A1_2O_3$ reaction at pH 6 is −2.56 V MSE.[19] Similar current transients have been observed during scratching of various metals at low potentials.[20] As a result of this superposition, both the negative and positive current responses are net signals, and the individual peaks are less than the observed peak values. Nonetheless, the cathodic portion of the curve in Fig. 5 exhibits a limiting current density of almost 30 A/cm^2. The rate of water decomposition, the dominant cathodic reaction, may be limited in the microsecond time scale by atomic hydrogen blocking part of the surface. Since the peak currents are much lower (in absolute value) than the anodic peak currents measured at higher potentials, ohmic considerations are small.

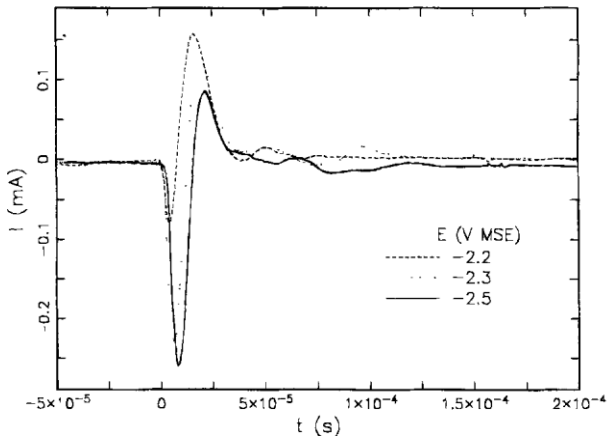

Fig. 10. Initials portion of current transients measured at low potentials in 1.2*N* K_2SO_4.

The IR-corrected data in Fig. 5 (filled circles) represent a sort of polarization curve for the bare metal area. As discussed above, the anodic current densities at each potential in the figure are likely to be lower than the true instantaneous bare metal reaction rate because of the rapid repassivation. Similarly, the cathodic current densities in the figure are somewhat less negative than the true values because of the superimposed anodic signal. Nonetheless, the limiting nature of the cathodic reaction at low potentials suggests that the instantaneous corrosion rate of the fresh metal area exposed at open circuit is controlled by the rate of the cathodic reaction and will be equal to the value of the limiting cathodic current density, about 30 A/cm^2.

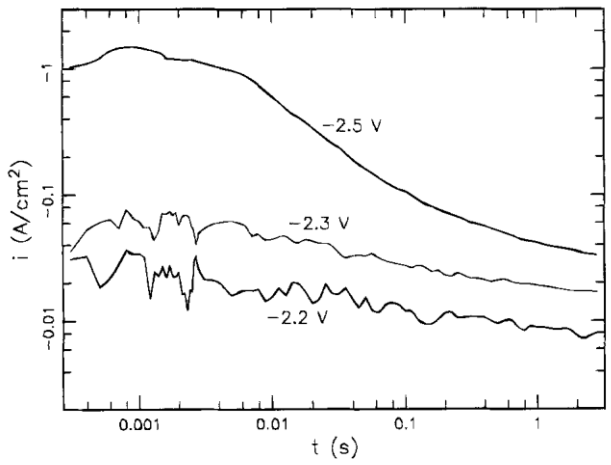

Fig. 11. Long-rime portions of current transients measured at low potentials in 1.2*N* K_2SO_4.

At longer times, after the anodic response becomes small, the net current becomes negative again, reaches a second maximum negative value, and then decays very slowly toward the background current. The final parts of the cathodic decay for the curves shown in Fig. 10 are given in Fig. 11. This transient form suggests that the rate of hydrogen evolution is faster on the fresh metal surface and decreases as the oxide film grows. The factors that limited current at very short times (perhaps blocking by hydrogen) are probably less important in the longer time scale given the low values of current. Furthermore, it can be assumed that by 1 ms the oxide film has formed sufficiently that bare metal area no longer exists. One possibility for explaining the slow decrease in cathodic current at long times is that the reaction is under activation control, with the activation energy dependent on the oxide film thickness because of tunneling of the current through the oxide. Electron tunneling through 20 to 30 A thick $A1_2O_3$ is possible and has been studied in some detail.[21] The tunneling current may be written as[22]

$$i_H = A \exp(-Bd) \qquad [1]$$

where i_H is the hydrogen evolution current density, d is oxide film thickness, and A and B are constants. Equation 1 may be written as

$$i_H = i_H^0 \exp(-q_p/q_p^0) \qquad [2]$$

where q_p is the charge consumed in film growth and i_H^O and q_p^0 are constants.

With the further assumption that oxide film growth at low potentials in the time range of interest follows direct logarithmic film-growth kinetics, it is possible to relate q_p, and thus i_H, to *t.* Direct logarithmic film growth dictates that[16]

$$i_p = C \exp(-Dq_p) \qquad [3]$$

where i_p is the current density going to passive-film formation and C and D are constants. Integrating Eq. 3 yields[17]

$$q_p = \frac{1}{D} \ln(DCt + 1) \qquad [4]$$

By fitting the data of Fig. 7 to Eq. 3, values of DC were found to be in the range of 5 to 12 × 10^6 s^{-1}. In the time range of interest ($t > 10^{-3}$ s), $DCt >> 1$, and Eq. 4 may be simplified to

$$q_p = \frac{1}{D} \ln (DCt) \qquad [5]$$

Rearranging Eq. 2 and equating to Eq. 5

$$-q_p^0 \ln (i_H/i_H^0) = \frac{1}{D} \ln (DCt) \qquad [6]$$

$$\ln (i_H) = \ln (i_H^0) - \frac{1}{Dq_p^0} \ln (DC) - \frac{1}{Dq_p^0} \ln (t) \qquad [7]$$

With the assumption that hydrogen evolution is limited by electron tunneling through an oxide film that is growing by direct logarithmic kinetics, a plot of ln i_H *vs.* 1n t should be linear, which is roughly observed in Fig. 11 for the transients at −2.2 and −2.3 V. The transient at −2.5 V has somewhat more curvature. The analysis assumes that there is no appreciable contribution of anodic current in this time regime. Nonetheless, both the anodic and cathodic extended current transients appear to support oxide growth by direct logarithmic kinetics.

Comments on the Breaking Electrode Technique

Microelectrodes have been used extensively in the past to reduce ohmic drops and increase mass-transport rates.[23-25] In this work, a thin film stripe deposited on an insulating substrate was broken to create a small fresh metal area very quickly. The speed of area creation brings the measurement of repassivation current into a new regime, shorter times and higher current densities, than previously accessed. This capability, however, generates certain problems. The voltage available to drive the interfacial faradaic reaction, V_f, at a bare surface is

$$V_f = V - IR \qquad [8]$$

where I is the current flowing and R is the approach resistance to the electrode. V is the applied overpotential and is equal to the difference between the applied potential and the reversible potential for the reaction. Since it is not reasonable for V_f to be negative, the maximum current, I_{max}, that can flow from the electrode through the solution resistance of a given value R is

$$I_{max} = \frac{V}{R} \qquad [9]$$

The approach resistance R to an electrode in an insulating plane is inversely proportional to a length parameter x, where x is the length of a rectangular electrode[13] or the radius of a disk[26]

$$R = \frac{R'}{x} \qquad [10]$$

where R' is a constant. The maximum achievable current density is given by I_{max} /A.A is the area of the electrode and is given by A′x^2 where A′ is a constant. Thus

$$i_{max} = \frac{V}{R'A'x} \qquad [11]$$

While Eq. 11 demonstrates that the accessible current densities increase with decreasing electrode size, *x*, Eq. 10 shows that the approach resistance also increases correspondingly. It is therefore impossible completely to avoid ohmic resistance effects by using microelectrodes. Even if the anomalously high resistance observed at the time of the peak currents could be reduced in the breaking electrode experiments, the higher resultant current would still generate a high ohmic potential drop. The motivation for making measurements at smaller electrodes with higher achievable current densities is the search for activation-limited kinetics, which were clearly not found in this case.

Since the ohmic potential drop was large and changing with time, the experiment was not strictly under potentiostatic control, and the surface potential was different from the set value at the short times. The response of the reference electrode and the potentiostat may be additional factors altering the potential of the surface at very short times.

An important observation from these experiments is that the interfacial faradaic reaction on bare Al surfaces is capable of supplying extremely large current densities. A practical implication is that the reaction of bare Al areas will never be under activation control. For instance, the reaction of the freshly created Al area at a crack tip, where geometrical constraints are certainly more severe than in the breaking electrode technique, will be limited by factors other than the activation kinetics of the bare surface, such as the ohmic resistance in the crack electrolyte.

The high currents measured at the shortest times and influenced by ohmic effects result in another problem of how to handle the large dynamic range of the current signal. In order to accommodate the current flow in a manner that maintains the best control of the system, a high current scale and a small measuring resistor are required. This limits the resolution at longer time periods (greater than milliseconds) when the current is quite small. Considering that the shortest times are dominated by ohmic effects, we have chosen to address the problem of the large dynamic current range by using a lower current scale and allowing the potentiostat to overload and lose control at very short times. The coincidence of the signal with that obtained using a higher current scale justifies this approach. The current observed after the oscillations have ceased provides a relatively large portion of the repassivation reaction in a time when other techniques are still incrementally creating a new area.

In order to use this technique, the material under study must be in the thin-film form, which limits it to certain systems. However, it provides an understanding of the limiting factors at very short times and the capability for observing repassivation kinetics at shorter times than other techniques.

Conclusions

Current transients measured on fresh Al surfaces were studied using the breaking-electrode technique. Both the peak current density in the microsecond time scale and the extended current decay over the period of 0.1 ms to 3 s were measured as a function of potential in 1.2*N* K_2SO_4, and the following was observed:

1. At high potentials the peak current density was limited by an ohmic resistance that was higher than that measured long after breaking.

2. The current decay observed in the range of 0.1 ms to 3 s is best represented by direct logarithmic film growth kinetics.

3. Complex cathodic transients observed at low potentials indicate that hydrogen evolution is enhanced on fresh metal surfaces and slows as an oxide forms and thickens.

4. A limiting peak cathodic current density of 30 A/cm^2 was observed at low potentials, and this current density may be considered to be the instantaneous corrosion current density for a fresh metal area at open circuit.

Acknowledgments

The authors gratefully acknowledge helpful discussions with H. Isaacs and T. Moffat. A.J.D. is supported by DOE Basic Energy Sciences under Contract No. DE-AC02-76CH00016.

IBM T.J. Watson Research Center assisted in meeting the publication costs of this article.

REFERENCES

1. G. S. Frankel, B. M. Rush, C. V. Jahnes, C. E. Farrell, A.J. Davenport, and H. S. Isaacs, *This Journal*, **138**, 643 (1991).
2. T. R. Beck, *ibid.*, **115**, 890 (1968).
3. T. R. Beck, *ibid.*, **120**, 1310 (1973).
4. T. R. Beck, *Corrosion*, **30**, 408 (1974).
5. R. P. Wei, M. Gao, and P. Y. Xu, *This Journal*, **136**, 1835 (1989).
6. T Hagyard and J. R. Williams, *Trans. Farad. Soc*, 57, 2288 (1961).
7. T. Hagyard and W. B. Earl, *This Journal*, **114**, 694 (1967).
8. G. T. Burstein and D. H. Davies, *ibid.*, **128**, 33 (1980).
9. G. T Burstein and P. I. Marshall, *Corros. Sci.*, **23**, 125 (1983).
10. P. D. Bastek, R. C. Newman, and R. G. Kelly, *This Journal*, **140**, 1884 (1993).
11. G. T. Burstein and R. J. Cinderey, *Corros. Sci.*, **32**, 1195 (1991).
12. G. T. Burstein and R. J. Cinderey, *ibid.*, **33**, 475 (1992).
13. H. J. Pearson, G. T. Burstein, and R. C. Newman, *This Journal*, **128**, 2297 (1981).
14. P.D. WashabaughandW G. Knauss,*Int. J. Frac*, **65**, 97 (1994).
15. N. Cabrera and N. F. Mott, *Rep. Prog. Phys.*, **12**, 163 (1948/49).
16. N. Sato and M. Cohen, *This Journal*, **111**, 512 (1964).
17. J. Kruger and J. P. Calvert, *ibid.*, **114**, 45 (1967).
18. G. T Burstein and A. J. Davenport, *ibid.*, **136**, 936 (1989).
19. M. Pourbaix, *Atlas of Electrochemical Equilibria in Aqueous Solutions*, NACE, Houston, TX (1974).
20. A. J. Davenport, Ph.D. Thesis, University of Cambridge, Cambridge, England (1987).
21. J. Lambe and R. C. Jaklevic, *Phys. Rev.*, **165,**821 (1968).
22. T. P. Moffat, H. Yang, E F. Fan, and A. J. Bard, *This Journal*, 139, 3158 (1992).
23. K. R. Wehmeyer, M. R. Deakin, and R. M. Wightman, *Anal. Chem.*, 57, 1918 (1985).
24. R. T. Atanasoski, H. S. White, and W. H. Smyrl, *This Journal*, **133,** 2435 (1986).
25. S. Pons and M. Fleishmann, in *Ultramicroelectrodes*, M. Fleishmann, S. Pons, D. R. Rolison, and P. P. Schmidt, Editors, Datatech Systems, Inc., Morgan-ton, NC (1987).
26. J. Newman, *This Journal*, **113,** 510 (1966).